Investigation of remaining tritium in the LHD vacuum vessel after the first deuterium experimental campaign

メタデータ	言語: English 出版者: 公開日: 2022-08-03 キーワード (Ja): キーワード (En): 作成者: MASUZAKI, Suguru, OTSUKA, T, OGAWA, Kunihiro, YAJIMA, Miyuki, TOKITANI, Masayuki, ZHOU, Q, ISOBE, Mitsutaka, OYA, Yasuhisa, YOSHIDA, N, NOBUTA, Yuji, The LHD Experiment Group メールアドレス: 所属:
URL	http://hdl.handle.net/10655/00013430

This work is licensed under a Creative Commons Attribution-NonCommercial-ShareAlike 3.0 International License.

Investigation of the distribution of remaining tritium in divertor in LHD

S. Masuzaki[1,2], M. Yajima[1,2], K. Ogawa[1,2], G. Motojima[1,2], M. Tanaka[1,2], M. Tokitani[1,2], M. Isobe[1,2], T. Otsuka[3] and the LHD Experiment Group

[1]*National Institute for Fusion Science, Oroshi 322-6, Toki 509-5292, Japan*
[2]*The Graduate University for Advanced Studies, SOKENDAI, 322-6 Oroshi-cho, Toki 509-5292, Japan*
[3]*Kindai University, 3-4-1 Kowakae, Higashi-Osaka, 577-8502, JAPAN*
(Received day month year / Accepted day month year should be centered 10-point type)

Abstract

To reveal the triton transport and the tritium migration in a deuterium plasma experiment in the Large Helical Device (LHD), the distribution of the remaining tritium in divertor tiles made of graphite after the first deuterium plasma experimental campaign in 2017 was investigated. In this study, tritium contents in divertor tiles have been measured by using a full-combustion method. The asymmetric tritium retention in divertor tiles located at symmetric positions, which was found in the previous study by the surface tritium measurement using an imaging plate technique, has been confirmed by the results of the full-combustion method. The asymmetry is considered to be attributed to the asymmetric distribution of lost-points of energetic tritons in divertor. A depth profile of remaining tritium in a divertor tile estimated by using a combination of the imaging plate technique and a sputtering treatment shows that the peak of the profile locates at several micro-meters from the surface. This result suggests that the majority of the remaining tritium impinged upon the divertor tile as energetic tritons. In this study, a distribution of lost-points of energetic tritons has been calculated by using a Lorentz orbit following code (LORBIT) with taking into account divertor components. The obtained distribution has been compared with measured tritium distributions on divertor tiles. The measured and calculated distributions are similar to each other, but they are not the same. The difference between them can be attributed to plasma exposures during and after the deuterium plasma campaign.

Keywords: tritium measurements, LHD, Lorentz orbit following code, full-combustion method, imaging plate technique

Highlights:

- The distribution of the remaining tritium in divertor tiles made of graphite after the first deuterium plasma experimental campaign in 2017 have been investigated by using a full-combustion method, the tritium imaging plate technique, and the Lorentz orbit following code (LORBIT) with taking into account divertor components.
- A depth profile of remaining tritium in a divertor tile estimated by using a combination of the imaging plate technique and a sputtering treatment suggests that the source of the remaining tritium is energetic tritons which were lost on the tile.
- The asymmetric tritium retention in divertor tiles located at symmetric positions, which were found in the previous study by using the imaging plate technique, has been confirmed by the results of the full-combustion method.
- The asymmetry is considered to be attributed to the asymmetric distribution of lost-points of energetic tritons in divertor.
- A distribution of lost-points of energetic tritons on a divertor tile calculated by using the LORBIT code and measured distributions of remaining tritium on the tile are compared.

1. Introduction

In a deuterium plasma in a fusion device, deuterium-deuterium (D-D) nuclear fusion reactions generate tritons with kinetic energy of 1.01 MeV. A portion of generated tritons is lost promptly to plasma facing components such as first wall and divertor tiles without collisions with background plasma particles. In large tokamaks such as JT-60U [1], JET [2], and TFTR [3], the portion is reported to be approximately 10 % - 50 % with depending upon operational magnetic configurations and plasma current. On the other hand, tritons with collisions are sufficient to be thermalized flow to the divertor with the background plasma. It is worth analyzing the amount and distribution of the remaining tritium in plasma facing components from viewpoints of understanding of tritium migration in a vacuum vessel of a fusion device, and safety of in-vessel works. Many studies of tritium distribution in plasma facing components after deuterium plasma experiments have been conducted in tokamaks by using a full-combustion method [4], the tritium imaging plate (IP) technique [5], and an accelerator mass spectrometry [6]. It has been revealed by these previous studies that a distribution of tritium content in plasma facing components fundamentally depends upon distribution of lost energetic tritons upon the components in the case of deuterium plasma experiments.

In the Large Helical Device (LHD), which is one of the world's largest superconducting stellarator / heliotron - type devices

with a major radius and a minor radius of 3.9 m and 0.6 m, respectively [7], deuterium plasma experiments have been conducted since 2017 [8], and this is the first opportunity for stellarator / heliotron devices to investigate tritium related issues.

During deuterium plasma experiments, high-energy tritons with kinetic energy of 1.01 MeV were generated by one of two deuterium-deuterium fusion reactions. In the case of LHD, the fusion reactions occurred mainly between neutral beams and thermal plasma ions. The portion of prompt loss of tritons was calculated by using a Lorentz orbit following code (LORBIT), and the result of the calculation shows that the portion is approximately 40 % in the case of the standard magnetic configuration (major radius of the magnetic axis, R_{ax}, is 3.6 m, magnetic field strength, B_t, is 2.75T), and energetic tritons lost between helical coil cans, that is, in helical divertor region [9]. On the other hand, evacuated gas analyses [10, 11] showed that approximately 35.5 % of the generated tritium was evacuated in the first deuterium plasma experimental campaign [10]. These results suggest that more than 60 % of the generated tritium could remain in the vacuum vessel, primarily in the helical divertor region.

The first experimental investigation of remaining tritium in plasma facing components in LHD was conducted using the tritium IP technique [13]. The results of the investigation show that the remaining tritium densities in divertor tiles made of graphite are much larger than those in the first wall panels made of stainless steel (type 316 L), and the result of calculation using the LORBIT code is consistent with the remaining tritium distribution obtained by using the tritium IP technique [12].

However, the IP technique can detect tritium remaining within the depth shallower than the escape depth of β-rays from tritium decay. Therefore, quantitative analysis of remaining tritium in plasma facing components is necessary to reveal the tritium distribution in the LHD vacuum vessel with more accuracy than the estimation using only the IP technique.

In this study, a quantitative analysis of remaining tritium in divertor tiles has been conducted by using a full-combustion method. Amounts of remaining tritium on divertor tiles are compared to the lost-points distribution of energetic tritons calculated by using the improved calculation with the LORBIT code which takes into account divertor components. To estimate the incident energy of tritium on a divertor tile, depth profile measurement of remaining tritium in a divertor tile is also conducted.

2. Setup of analyses

In this section, the first deuterium plasma experimental campaign in LHD is briefly mentioned. Then, analyzed divertor tiles in this study, analyses of a depth profile of remaining tritium in a divertor tile, and tritium content in a sample cut from the

divertor tiles are explained. The calculation of lost-points of tritons on plasma facing components using the LORBIT code is also mentioned.

2.1. *The first deuterium plasma experimental campaign in LHD*

The first deuterium plasma experimental campaign was conducted in 2017 for four months after one month of the hydrogen plasma experimental campaign. Plasma was generated and heated by electron cyclotron resonance heating (ECRH) and neutral beam injections (NBIs). The ECRH system consisted of three 77 GHz gyrotrons and two 154 GHz gyrotrons, and the total heating power was up to 5.4 MW. The NBIs consisted of three tangentially injected NBs with the beam energy of 180 keV and two perpendicularly injected NBs with the beam energy of 40 – 80 keV [8]. The total port-through power of NBIs was up to 31 MW. The deuterium plasma campaign was followed by one month by the hydrogen plasma campaign, eleven days of mild temperature (95 °C) baking and hydrogen glow discharges (total 44 h) to reduce tritium content in plasma facing components.

In LHD, plasma experiments are conducted under the helical divertor configuration [13]. Figure 1(a) shows divertor tile arrays in one half of a torus. The red and blue colored divertor tile arrays in Fig. 1(a) are expanded in Fig. 1(b). An inboard-side divertor is a "closed" divertor equipped with the "dome," which is the green colored component in Fig. 1(b). Figure 1(c) shows a cross-sectional view of an inboard-side divertor in a plane perpendicular to helical coils at around the equator.

Divertor components, dome, and divertor tiles are typically made of isotropic graphite (IG-430U, TOYO-Tanso), while the plasma facing material of first wall panels is stainless steel (type 316 L).

2.2. *Analyzed divertor tiles*

In the previous study [12], it was revealed that energetic tritons were lost primarily in the inboard-side divertor. Therefore, in this study, two divertor tiles, RD16 and LD17 (I-3R and I-3L, in [12]), retrieved from the inboard-side divertor were analyzed. They were located at a symmetric position near the equator as shown in Fig. 1(b) at the toroidal section of 9. Each divertor tile consists of the "baffle part" and the "divertor trace part," as shown in Fig. 2(a). Divertor trace basically locates on the divertor trace part, and as a result, erosion and deposition are significant on the divertor trace part as shown in Fig. 2(b). A microstructure observation of cross-sectional specimen cut from the divertor tiles by using a focused ion beam fabrication shows deposition layers with thickness of less than 100 nm and approximately 10 μm exist on the samples of the "baffle part" and the "divertor trace part," respectively.

Figure 2(c) and (d) show distributions of photo-stimulated luminescence (PSL) intensity on RD16 and LD17, respectively, measured by using the IP technique. PSL intensity can be considered to be proportional to tritium content within the escape depth of β-rays from tritium decay. It is clearly shown that tritium content within the escape depth in the baffle part is larger

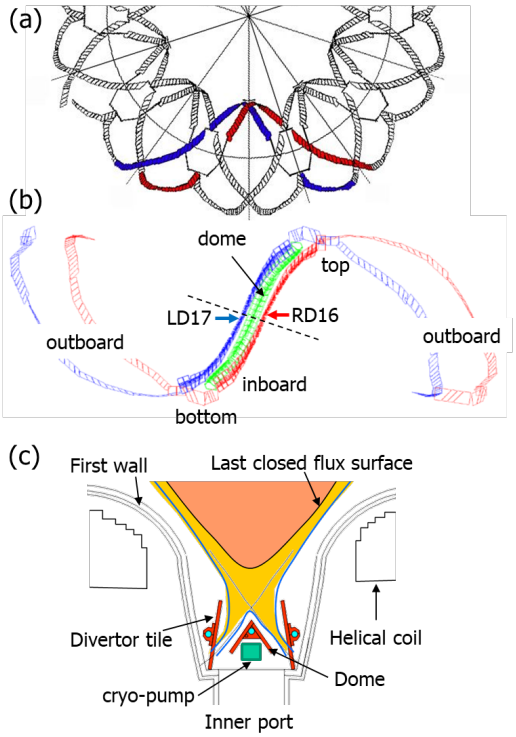

Fig. 1 (a) Divertor tile arrays in the helical divertor in LHD, (b) Red and blue colored divertor tile arrays in (a) showing positions of retrieved divertor tiles (RD16 and LD17) for this study, (c) cross-sectional view of an inboard-side divertor in a plane perpendicular to helical coils at the position of the dashed line in (b).

than that in the divertor trace part in the case of each tile. On the other hand, tritium content within the escape depth is similar on the divertor trace part of these tiles.

Retrieved tiles were cut into small samples for analyses. Samples for the measurement of depth profile of remaining tritium, which is mentioned in the next section, were cut from RD16 as shown in the insertion in Fig. 5, and the size of samples is approximately 15 × 15 × 7 mm^3. Samples for tritium content measurement were cut along the red colored dashed lines in Fig. 2(c) and (d), and their size is approximately 15 - 25 × 5 × 1 mm^3.

2.2. *Combination analysis with IP and a sputtering treatment*

To analyze the depth profile of remaining tritium in a divertor tile, a combination analysis using the IP technique and a sputtering treatment were conducted. For the sputtering treatment, a glow discharge emission spectroscopy [14] device (GDA750, Rigaku) was utilized. In the device, a surface of a sample works as a cathode of a RF-glow discharge. The diameter of the plasma column in the glow discharge was 4 mm in this study. A sample surface was sputtered by argon ion bombardments. Five samples cut from the RD16 tile as shown in Fig. 5 were treated with different discharge times from 100 s to 1000 s. After the treatment, a crater was formed by erosion with sputtering. Depths of craters were measured by using a profilometer with a

stylus. Then the IP technique was applied to the five treated samples.

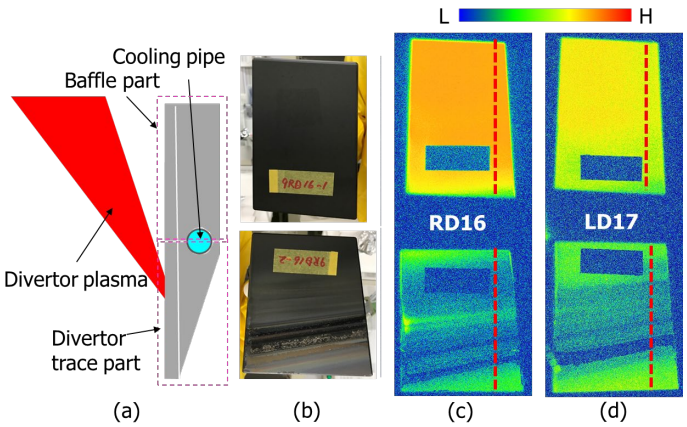

Fig. 2 (a) A schematic side view of a divertor tile in a closed divertor, (b) photo of the RD16 tile (top: baffle part, bottom: divertor trace part), distributions of the PSL intensity on the RD16 (c) and the LD17 (d) tiles, respectively, measured by the imaging plate technique. Red dashed lines show that samples for the combustion method were cut along these lines. Profiles of PSL intensity in Fig. 6 are also along these lines.

2.3. *Full-combustion method*

To measure remaining tritium contents in samples cut from divertor tiles, a full-combustion method was conducted. Figure 3 shows the scheme of the full-combustion method in this study. A quartz tube with inner diameter of 16 mm, and 300 mm long surrounded by an electric heater was utilized as a reactor. A thermocouple touched the outside of the tube to monitor the temperature of a sample in the tube. From the upstream of the reactor, moist air flew into the reactor with the flow rate of 300 SCCM, and then, air including tritium flew into an oxidation reactor with two palladium catalysts as shown in Fig. 3. The catalyst is supported on a metal honeycomb [15], and was heated by a heater to 668 K to oxidize tritium in chemical forms of tritiated hydrogen gas and tritiated hydrocarbons into tritiated water vapor. The tritiated water was collected by water bubblers,

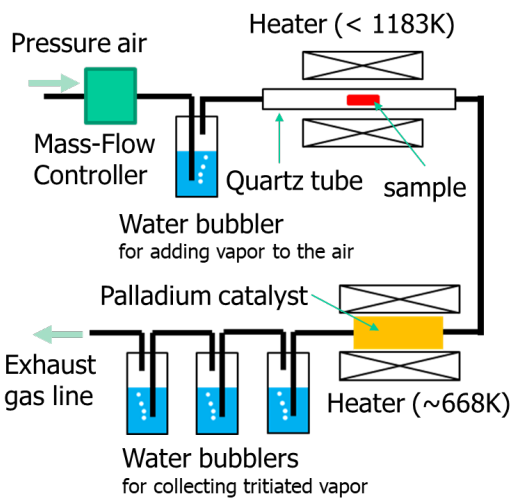

Fig. 3 A scheme of the combustion method.

in which 15 ml of pure water was contained as shown in Fig. 3. At each bubbler, the tritiated water was collected with the collection rate of more than 99 %. A sample placed on an alumina boat was inserted into the tube, and was heated up to 1183 K with taking approximately 30 min. The temperature was kept for 10 min. to 30 min. to maintain combustion of a sample, and then, heater was turned off. From each bubbler, 10 ml of water was sampled, and was mixed with 10 ml of liquid scintillator in a polyethylene vial, and the tritium activity was determined by a liquid scintillation counter. Metallic deposits, which deposited on the plasma facing surface of a divertor tile during glow discharges and plasma experiments, remained on the alumina boar after the combustion operation. It was confirmed by thermal desorption in the same experimental setup as the combustion method that the remained deposits contained tritium less than the amount detectable by the liquid scintillation counter.

2.4. *Orbit calculation for tritons*

Losses of energetic tritons generated by D-D reactions occur due to collision-less orbit loss, reaching the loss cone and charge-exchange reaction with low energy neutral particles. The orbit calculation for tritons generated in the core plasma is carried out by using the LORBIT code, which is a Lorentz orbit following code. In this study, the calculation was conducted with taking into account divertor components such as divertor tiles and dome. This is an improved point from the previous study [12].

A neutral beam heated plasma in the standard magnetic configuration (R_{ax} = 3.6 m, B_t = 2.75 T) was considered. The assumed line-averaged electron density, and electron and ion temperature were 2×10^{19} /m^3, and 3 keV. The distribution of points of triton generation was calculated by using FIT3D-DD code [16].

3. Results and discussions

In this section, results of analyses are mentioned and discussed. First, the calculated distribution of lost points of energetic tritons on plasma facing components is mentioned. Then, the depth profile of the remaining tritium in the divertor tile, RD16, retrieved from near the equator is considered from the result of the combination analysis, and incident energy of tritons are discussed. The remaining tritium content in the RD16 and in the LD17 tiles measured by using the combustion method are shown, and these results are compared to results of measurements using the IP technique, and the calculated distribution of lost points of energetic tritons on the tiles.

3.1. *Lost points of energetic tritons on plasma facing surfaces*

In the previous study, the calculation of lost points of energetic tritons did not take into account divertor components. In this study, the calculation was improved to take into account the components. Figure 4 (a) shows the distribution of lost

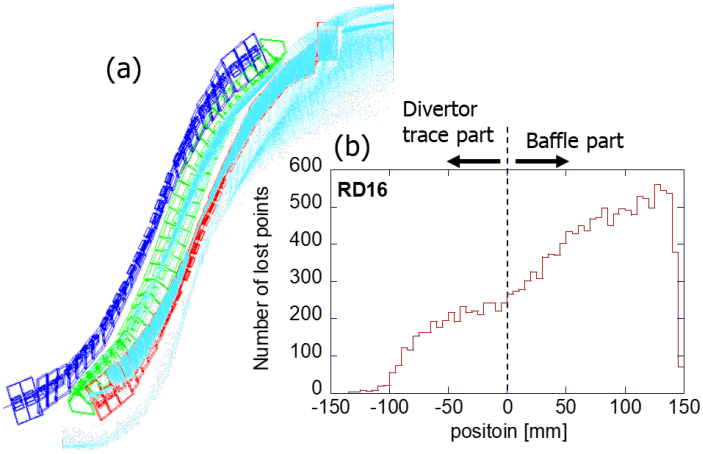

Fig. 4 (a) Lost points on plasma facing surfaces at torus inboard-side for the case of the direction of the toroidal field of counter clock-wise direction (CCW B_t). Components drawn by blue, green, and red are divertor components shown in Fig. 1(b). Light blue dots are lost points of energetic triton. Divertor components are drawn as line drawing. (b) Profile of the number of lost points of energetic triton on the RD16 tile in the case of the CCW B_t.

points of energetic tritons on plasma facing components at an inboard-side. A major part of lost points appears on the red colored divertor tiles, while no lost point is on the blue colored divertor tiles. This is attributed to that drift is an important process of energetic triton loss without collisions [9, 12]. Energetic tritons were also lost on top of dome components, and first wall near the red colored divertor tiles.

Figure 4(b) shows a profile of the number of lost points of energetic tritons on the RD16 tile in the case of the toroidal field of counter clock-wise direction (CCW B_t). Approximately 78 % of lost points of tritons on this tile is on the baffle part. This result is consistent with the results of the IP measurement shown in Fig. 2 (c) and (d). In the case of the toroidal field of clock-wise direction (CW B_t), the profile of the number of the lost points on the LD17 tile is the same as Fig. 4(b).

3.2. *Depth profile of remaining tritium in the divertor tile*

In Fig. 5(a), two-dimensional tritium distribution on the surface of the baffle part of the RD16 tile. Samples for the combination analysis were cut from the baffle part as shown by dashed lines in the insertion. Tritium distributions on two samples after the sputtering treatment are also shown in the insertion. The times of treatment for these samples were 420s and 1000s. It is clearly observed that the areal densities of remaining tritium inside the sputtered areas on samples are different from the areal densities on no-treated surfaces.

Figure 5(b) shows the depth profiles of normalized PSL intensity which is the ratio of a PSL intensity inside a crater and PSL intensity on a no-treated surface around the crater by red symbols and an emission line intensity of deuterium.

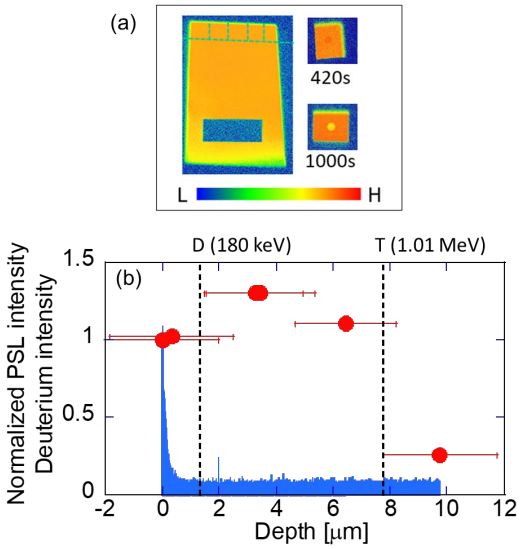

Fig. 5 (a) Distributions of PSL intensity on the baffle part of the RD16 tile (left), samples after 420 s and 1000 s of the sputtering treatment. The diameter of a sputtered crater is 4.0 mm. Samples were cut from the baffle part of the RD16 tile as shown by dashed lines. (b) Depth profile of the PSL intensity (red symbols) and deuterium (blue area) in the baffle part of the RD16 tile measured by using the combination of IP and the sputtering treatment. For the PSL intensity, error bars show the standard deviation of the depth data. Black dashed lines show range of deuterium (D) with kinetic energy of 180 keV and tritium (T) with kinetic energy of 1.01 MeV, respectively.

Horizontal error-bars are standard deviation of depth data which is attributed to the surface roughness for a porous structure of isotropic graphite. It is clearly shown that the peak of the depth profile of the PSL intensity locates between 3 - 6 μm from the surface which is much deeper than the deposition layer formed on the surface of this sample. It should be noted here again that an IP for tritium measurement can detect β-rays from tritium decay within a depth shallower than the escape depth of the β-rays. The maximum escape depth for β-rays from tritium with maximum energy of 18.6 keV is approximately 3 μm for the case of graphite [17]. For the shallow escape depth of β-rays from tritium decay, the peak of remaining tritium can be considered to locate at deeper than the peak of the profile of the PSL intensity. In Fig. 5(b), ranges of normal incident deuterium and tritium with kinetic energy of 180 keV and 1.01 MeV, respectively, in graphite calculated by using SRIM code [18] are shown by black dashed lines, respectively. The former energy is the negative ion base neutral beam energy in LHD, and the later energy is the same as a generated triton by a D-D reaction. The peak of remaining tritium in the divertor tile is much deeper than the range of deuterium with incident energy of 180 keV, and shallower than the range of hydrogen with incident energy of 1.01 MeV. From these results, the origin of the remaining tritium in the baffle part of the RD16 tile can be concluded to be energetic tritons lost to the divertor tile with shallower incident angles than normal incidence. The depth profile of deuterium shown in Fig. 5(b) by the blue area shows that deuterium is remaining in the range less than 400 nm from the surface, and the range is much less than that of tritium.

3.3. *Profiles of remained tritium in the divertor tiles*

Figure 6 (a) and (c) show profiles of remained tritium content in the RD16 and the LD17 divertor tiles, respectively, obtained by the combustion method. Measured samples were cut along red dashed lines shown in Fig. 2 (c) and (d). The unit of vertical axes of these graphs is areal density, which is defined to be the remained tritium content divided by plasma facing areas of samples. In both divertor tiles cases, the largest areal density is observed in the yellow hatched part, that is, the baffle part, and the largest areal density observed on the RD16 and the LD17 tiles are 0.51 GBq/m^2 (2.84 × 10^{17} T/m^2) and 0.06 GBq/m^2 (0.33 × 10^{17} T/m^2), respectively. The asymmetry observed by the IP measurements is clearly observed in results of the combustion method.

Profiles of PSL intensity along the same red dashed lines in Fig. 2 (c) and (d) are also shown in Fig. 6 (b) and (d), respectively. These profiles are not the same as profiles of areal density, but are similar to them. For both the RD16 and the LD17 cases, profiles of areal density and PSL intensity show that remained tritium content decreases from the baffle part to the divertor trace part, and remained tritium content in the divertor trace parts are much smaller than that in the baffle parts.

These experimentally obtained profiles are compared with the profile of the number of lost points of energetic tritons obtained by the calculation using the LORBIT code shown in Fig. 4 (b). In the calculated profile, the number of lost points decreases from the baffle part to the divertor trace part as with the profiles obtained experimentally shown in Fig. 6. On the other hand, the slope of the decrease is more gradual in the case of Fig. 4 (b) than experimental results shown in Fig. 6, and the ratio of number of lost points on the divertor trace part to that on the baffle part is larger than the ratios of areal density and PSL intensity. A possible reason for this discrepancy is that divertor plasma exposure during the deuterium plasma campaign and followed hydrogen plasma campaign reduced tritium content in the divertor trace parts.

Insertions in Fig. 6 (a) and (b) are areal density and PSL intensity on the divertor trace part of the RD16 tile with the same vertical axes as Fig. 6 (c) and (d), respectively. It is interesting that areal density and PSL intensity on the divertor trace parts of the RD16 are similar to them on the LD17, though areal density and PSL intensity on the baffle part on the RD16 tile are approximately six times larger than those on the LD17 tile. Here again, plasma exposure during the deuterium plasma campaign and followed hydrogen plasma campaign can be the cause of this result. Asymmetry is not only in energetic tritons, but also in the divertor plasma flow for drifts which depend on the B_t direction [12, 19]. For the CCW B_t case, larger heat and particle fluxes come to divertor tiles in the red colored array in Fig. 1(b). After the deuterium plasma experimental campaign, a hydrogen plasma experimental campaign followed for one month. During the hydrogen plasma campaign, 64 % of experiments were conducted with the CCW B_t. It can be speculated that tritium content in divertor tiles could asymmetrically reduce during the hydrogen plasma campaign, and as the result, tritium content in divertor trace parts of the RD16 and the LD17 are similar.

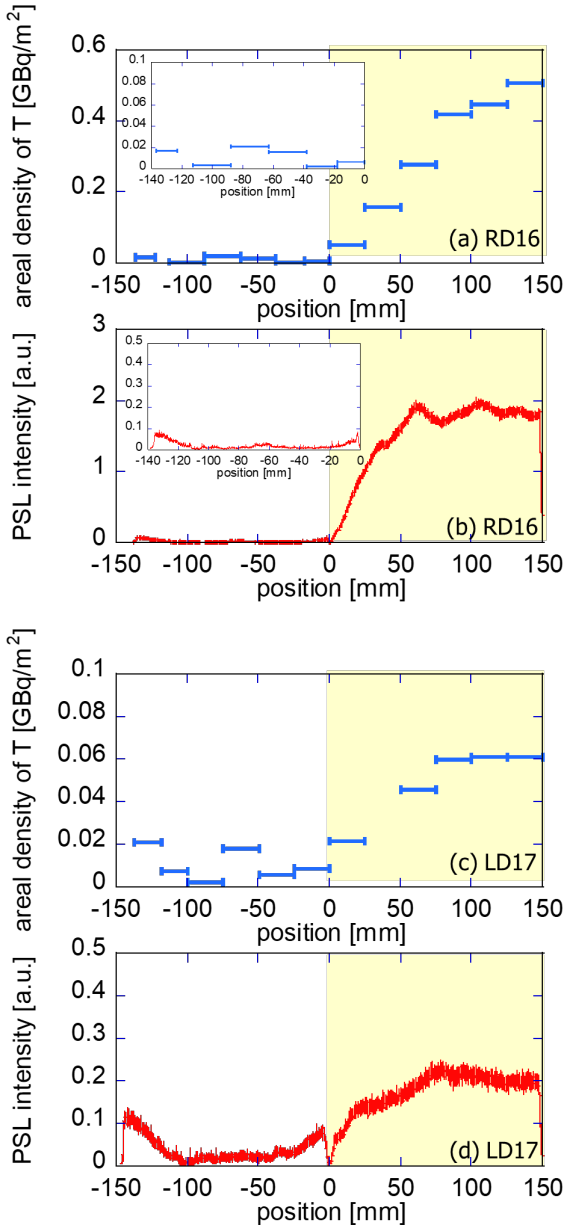

Fig. 6 Profiles of areal density of remained tritium measured by using the combustion method are shown by blue bars, which show widths of samples, on the R16 (a) and the LD17 (c) tiles. Red lines show profiles of amounts of surface tritium shown by PSL intensity measured by using the IP technique on the RD16 (b) and the LD17 (d) tiles. In each graph, the hatched part is the baffle part, and the white part is the divertor trace part. Insertions in (a) and (b) are the enlarged plot of the areal density and the PSL intensity on the divertor trace part of the RD16 tile for comparisons with profiles for the LD17 tile.

3.4. *Quantitative comparison of remained tritium contents estimated by experimental and calculated results*

Total amount of remained tritium in the RD16 and the LD17 tiles can be estimated by using results of the analysis using the combustion method. The total amount is approximately 4.8 MBq (2.70×10^{15} T) and 0.9 MBq (5.09×10^{14} T), respectively.

The remaining tritium measurements were conducted approximately three years after the end of the first deuterium plasma experimental campaign, and the tritium decay must be considered. Assuming the half decay period of tritium to be 12.3 years, approximately 15 % of remained tritium in the tiles decayed. With considering the estimated tritium decay, the remained tritium in the RD16 and LD17 tiles at the end of the first deuterium experimental campaign were approximately 5.5 MBq (3.11×10^{15} T) and 1.1 MBq (5.85×10^{14} T), respectively.

Although plasma exposures during and after the deuterium plasma experimental campaign affect the tritium content in divertor tiles, it is worth comparing the experimentally estimated tritium contents in the RD16 and the LD17 with the estimated numbers of energetic tritons lost on the tiles by using results of the LORBIT calculation. The total amount of generated tritons during the first deuterium plasma experimental campaign in LHD was approximately 6.4 GBq (3.6×10^{18} T), of which approximately 5.8 GBq (3.2×10^{18} T) were generated in the experimental condition of the CCW B_t, and the rest were generated in the condition of the CW B_t. In the calculation with the LORBIT code, approximately 5.9×10^5 particles were traced, and approximately 1.9×10^3 particles of the traced particles were lost to the RD16 tile. From these numbers, lost tritons on the RD16 and the LD17 can be calculated with assumptions of no toroidal asymmetry, and of that 40 % of generated tritons were lost without collision. The result of the calculation is that approximately 7.4 MBq (4.1×10^{15} T) and 0.7 MBq (4.2×10^{14} T) were lost on the RD16 and the LD17 tiles, respectively. These numbers are the same order of magnitude as the estimated amount using the result of the combustion method. This result suggests the LORBIT calculation can be used for rough estimation of remaining tritium distribution.

3.5. *Effects of plasma exposures on tritium migration*

Effects of plasma exposures on tritium migration are discussed here. During the deuterium plasma experiment, energetic tritons impinge on plasma facing components, mainly divertor tiles. Simultaneously, deuterium ions come to divertor trace parts of divertor tiles with much higher flux, and shallower incident range than those of energetic tritons. Tritium in divertor tiles can desorb for recombination with deuterium atoms, and for thermal release caused by rising tile temperature. Desorbed tritium can be evacuated. On the other hand, tritium can be released as tritiated hydrocarbon for chemical sputtering, and hydrocarbon can deposit on the first wall. Results of the recent analysis of remaining tritium in material probes on first wall show that tritium content in probes depend upon thickness of deposition layer [19]. This suggests that tritium can migrate with eroded carbon from divertor tiles.

4. Summary

The measurements of remaining tritium in divertor tiles, RD16 and LD17, retrieved from a symmetric position after the

first deuterium plasma experimental campaign in LHD have been conducted by using the full-combustion method. An asymmetric remaining tritium in the divertor tiles was observed, which was also observed in the previous study with the IP technique, though it had not been clear whether the asymmetric tritium remaining is only for near surface or for total amount of remaining tritium. This asymmetry is attributed to the asymmetric loss of energetic tritons to plasma facing components caused by drifts.

The result of the combination analysis of the IP technique and the sputtering treatment shows the peak of the depth profile of remaining tritium in the baffle part of the RD16 divertor tile locates several micro-meters from the surface. This suggests the source of remaining tritium is energetic tritons.

Profiles of remained tritium content on the RD16 and the LD17 divertor tiles were obtained by the full-combustion method and the IP analysis. Profiles obtained by using these different techniques are similar to each other. Comparison of the profile of calculated lost points of high energy tritons on the RD16 tile and the profiles of remained tritium content has been conducted. Decrease of remaining tritium content from the baffle part to the divertor trace part is shown in all profiles. The slope of the profile obtained by the calculation is more gradual than slopes in experimentally obtained profiles, and expected remaining tritium content in the divertor trace part from the calculation is larger than experimental results. This can be attributed to the effects of plasma exposures during the deuterium plasma campaign and the following one-month hydrogen plasma campaign.

The result of quantitative comparison of remained tritium content in the divertor tiles and the calculated number of lost points of energetic tritons on the tiles shows that the calculation can be used for rough estimation of remaining tritium distribution.

Acknowledgments

S. M. is grateful for Prof. Y. Torikai for his practical advice for tritium measurements. S. M. is also grateful for H. Yonezu, C. Iwata and D. Nagata for their dedicated technical support. This study was partially supported by NIFS budget ULFF019, ULFF026, and UFFF039, and by a JSPS KAKENHI grant (18H01203).

References

[1] K. Masaki et al, J. Nucl. Mater. **313-316** (2003) 514.

[2] C.W. Barnes et al, Nucl. Fusion **38** (1998) 597.

[3] H. Sjöstrand et al, J. Phys. D: Appl. Phys. **41** (2008) 115208.

[4] M. Yoshida et al, Fus. Sci. Tech. **60** (2011) 1560.

[5] T. Tanabe, Tritium: Fuel of Fusion Reactors (Berlin:Springer) (2017).

[6] C.Stan-Sion et al, Fus. Eng. Des. **89** (2014) 2628.

[7] Y. Takeiri et al, Nucl. Fusion **57** (2017) 102023.

[8] H. Takahashi et al, Nucl. Fusion **58** (2018) 106028.

[9] K. Ogawa et al, Plasma Sci. Technol. **21** (2019) 025102.

[10] M. Tanaka et al, J. Nucl. Sci. Tech. **57** (2020) in press.

[11] M. Tanaka et al, Fusion Eng. Des. **127** (2018) 275.

[12] S. Masuzaki et al, Phys. Scr. **T171** (2020) 014068.

[13] G. Motojima et al, Nucl. Fusion **59** (2019) 086022.

[13] S. Masuzaki et al, Nucl. Fusion **42** (2002) 756.

[14] C.N. Taylor et al, AIP advances **7** (2017) 055305.

[15] M. Tanaka et al, J. Radioanal. Nucl. Chem. **318** (2018) 877.

[16] S. Murakami et al, Trans. Fusion Technol. **27** (1995) 259.

[17] J. Gledhill, J. Phys. A **6** (1973) 1420.

[18] J.F. Ziegler, J.P. Biersack and U. Littmark, The Stopping and Range of Ions in Solids (1985) (New York: Pergamon)

[19] M. Yajima et al, in this PSI conference.